

MSAS – Assignment #2: Modeling

Giovanni Chiarolla, 964831

1 Questions

Question 1

1) List the stages of dynamic investigation and their meaning. 2) When going from the *real system* to the *physical model* a number of assumptions are made; report the most important ones along with their mathematical implications. 3) For each of the assumptions below, shortly state what sort of simplification may result: i) The gravity torque on a pendulum is taken proportional to the pendulum angle θ ; ii) Only wind forces and gravity are assumed in studying the motion of an aircraft; iii) A temperature sensor is assumed to report the temperature exactly; iv) The pressure in a hydraulic actuator is assumed uniform throughout the chamber. 4) List the *effort* and *flow* variables for the domains treated and discuss their similarity.

1) The objective of the dynamic investigation is to study how different interrelated system change over time. There are three main phases of dynamic investigation: Modelling phase, Analysis phase and Synthesis phase. The modelling phase firstly analyzes the real system in order to make assumptions which are needed to produce the so called physical model. The physical model is an interpretation of the real system with a certain level of approximations. Once the physical model is derived, it is possible to generate the mathematical model which provides equations describing the behaviour of the physical model itself. During the analysis phase the differential equations of motion of the mathematical model are solved either numerically or analytically. The data retrieved by the differential equations are used to study the dynamic behaviour. The synthesis phase is the phase in which decisions are made, i.e. the modification of some physical parameters of the system and/or augment the system so that it behaves as desired. 2) There are several approximations that usually are used moving from real to physical model. Firstly neglecting small effects. It is an important engineering approximation since it generates simple systems with low variation on the system response with respect to the original system. It also generates a reduction of the variables associated to the system and a reduction of the complexity of the system itself. Another important assumption is to assume that the environment around the system is unaltered by the system itself. To simplify the system it is usually used the lumped parameter approach where distributed characteristics are replaced by lumped characteristics. The linearization of the system is an important approximation used during the definition of the physical model. It generates simple algebraic and/or differential equation, from which a simpler mathematical model is derived. Constant parameter assumption is usually used in order to simplify the overall system. Finally, uncertainties and noise are usually neglected in first analysis in order to avoid statistical models. 3) The oscillations of a pendulum depends on a sinusoidal function of the aperture angle θ . In case of small oscillation angles, during the analysis it is possible to assume a linearization of the $\sin(\theta) \approx \theta$. ii) The motion of an aircraft depends mainly on gravity and wind forces but also on other forces that are usually neglected. Those forces are: the solar wind pressure, the Earth magnetic field torque on aircraft and the Earth's gravity gradient. These forces are neglected due to the very low magnitude with respect to the Gravity and wind forces. iii) Sensors produce data which are sensible of errors. The errors are of two types: systematic and random. If the errors are taken into account, it is necessary to implement a statistical analysis of the data. In fact the temperature measurements depend on the accuracy and the precision of the sensor. The introduction of this approximation leads to a simpler analysis concerning a deterministic approach. iv) Actually the pressure inside the chamber varies while the hydraulic actuator changes its

position. This is due to the fact that the pressure gradient travels along the fluid with a finite period and generates a variation of pressure inside the chamber over time. 4) The list of effort and flow variables to be taken into account accordingly to the domain are collected in Tab.1.

Table 1: Effort and Flow variables depending on the domain.

Domain	Effort	Flow
Mechanical	Force	Velocity or Position
Thermal	Temperature	Heat flow
Fluid	Pressure	Volume flow rate
Electrical	Voltage	Current

The Systems similarity is related to the fact that modelling many different kinds of dynamic systems results in the same, or similar, differential equations. Also the way in which different systems handle energy is similar. They practically rely on dissipative elements (resistance), effort storage elements (capacitance) and flow storage elements (inductance). For this reason it is possible to use similar equations in different domains.

Question 2

1) Briefly discuss the physical meaning of the bulk modulus; show how the *effective* bulk modulus is computed. 2) Under what circumstances the fluid resistance yields a linear relation between effort and flow variables? 3) Find the expression of the leakage through a thin annular gap starting from the balance between shear stress and pressure drop.

The bulk modulus of a substance represents the measure of how resistant to compression that substance is. Eq.1 represent the bulk modulus, where (p_0, T_0) are the reference conditions.

$$\beta = \rho_0 \left(\frac{\partial p}{\partial \rho} \right)_{p_0, T_0} \quad (1)$$

Generally the bulk modulus is defined at constant temperature as the isothermal bulk modulus, but can also be defined at constant entropy as the adiabatic bulk modulus. It is possible to rewrite Eq.1 in a finite variation of the properties between two known points. The isothermal finite representation is represented by Eq.2

$$\beta = -V \frac{\Delta p}{\Delta V} \quad (2)$$

And the adiabatic finite representation is shown in Eq.3

$$\beta_a = k\beta \quad (3)$$

where k is the ratio between specific heat at constant pressure and specific heat at constant volume. The effective bulk modulus is defined since in real hydraulic systems there is always a low concentration of air. For this reason it is possible to define the following equation:

$$\Delta V_{tot} = -\Delta V_L - \Delta V_g + \Delta V_c \quad (4)$$

Where ΔV_{tot} is the variation of the total volume, $-\Delta V_L$ is the variation of liquid volume, $-\Delta V_g$ is the variation of the gas volume and ΔV_c is the variation of volume related to the container. The effective bulk modulus can be written in the following form:

$$\frac{1}{\beta_e} = \frac{\Delta V_{tot}}{V_{tot} \Delta p} \quad (5)$$

Substituting Eq.5 in Eq.4 it is possible to write the effective bulk modulus as function of the liquid bulk modulus, the gaseous bulk modulus and the container bulk modulus in Eq.6

$$\frac{1}{\beta_e} = -\frac{\Delta V_l}{V_{tot}\Delta p} - \frac{\Delta V_g}{V_{tot}\Delta p} + \frac{\Delta V_c}{V_{tot}\Delta p} \quad (6)$$

Since $V_l = V_t - V_g$ and assuming $\beta_l \simeq 210^3 \text{MPa}$ and $\beta_g \simeq 210^1 \text{MPa}$ and $\beta_l \gg \beta_g$, the effective bulk modulus can be represented by Eq.7.

$$\frac{1}{\beta_e} \cong \frac{1}{\beta_l} + \frac{V_g}{V_{tot}} \frac{1}{\beta_g} + \frac{1}{\beta_c} \quad (7)$$

2) There only two conditions under which the fluid resistance generates a linear relation between effort and flow variable. The first one is when the flow is completely laminar and the second one is when the fluid is flowing inside a circular annular gap. 3) For a thin annular gap with thickness e , clearance $g = 2e$, width πD and length L , it is possible to retrieve the leakage equation considering stationary conditions between pressure drop and shear stress:

$$2y\pi Dp = -2L\pi D\mu \frac{dv}{dy} \quad (8)$$

Integrating Eq.8 from y to $\frac{e}{2}$ with $v(\frac{e}{2}) = 0$, Eq.9 is obtained.

$$v(y) = \frac{\Delta p}{2L\mu} \left(\frac{e^2}{4} - y^2 \right) \quad (9)$$

Finally, the total flow is retrieved by integrating $dQ = v(y)\pi Ddy$ between $y = -\frac{e}{2}$ and $y = \frac{e}{2}$ as it follows:

$$Q = \int_{-e/2}^{e/2} \frac{\pi D \Delta p}{2L\mu} \left(\frac{e^2}{4} - y^2 \right) dy = \frac{\pi D \Delta p}{12L\mu} e^3 = \frac{g^3 \Delta p}{96L\mu} \pi D \quad (10)$$

Question 3

1) Derive from scratch the mathematical model for RC and RL circuits and express the system response in closed form. 2) Consider a real DC motor and a) sketch its physical model (list the assumptions made); b) derive its mathematical model; c) show how the motor constant depends on the physical parameters.

It is possible to obtain the mathematical model of the RC circuit in Fig.1 applying the capacitor's constitutive law in Eq.11, the Kirchhoff's laws in Eq.12 and the Ohm's law in Eq.13.

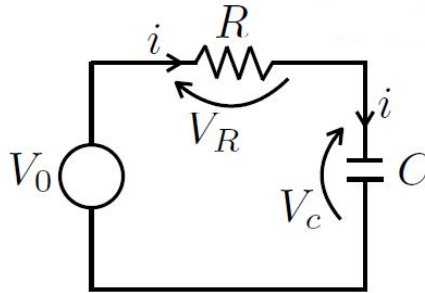


Figure 1: RC Circuit.

$$i_C = C \frac{dV_C}{dt} \quad (11)$$

$$V_R = V_0 - V_C \quad \text{and} \quad i_C = i_R \quad (12)$$

$$i_R = \frac{V_R}{R} \quad (13)$$

By Substituting Eq.11 and Eq.12 in Eq.13 the mathematical model which describes the RC circuit is retrieved (Eq.14).

$$\frac{dV_C}{dt} + \frac{V_C}{RC} = \frac{V_0}{RC} \quad (14)$$

Finally, the analytical solution of the ODE in Eq.14 is represented by Eq.14

$$V_C(t) = V_C(0) + V_0(1 - e^{-\frac{t}{\tau}}) \quad \text{with} \quad \tau = RC \quad (15)$$

The same procedure is applied to the RL circuit in Fig.3. It is defined the constitutive law of

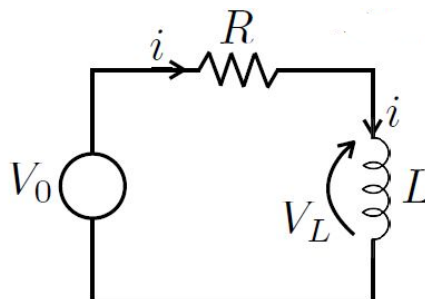


Figure 2: RL Circuit.

the inductor (Eq.16).

$$V_L = L \frac{di_L}{dt} \quad (16)$$

By Substituting Eq.16 and Eq.12 in Eq.13 the mathematical model which describes the RL circuit is retrieved (Eq.17).

$$\frac{di_L}{dt} + \frac{R}{L}i_L = \frac{V_0}{L} \quad (17)$$

Finally, the analytical solution of the ODE in Eq.17 is represented by Eq.18

$$i_L(t) = i_L(0) + \frac{V_0}{L}(1 - e^{-\frac{t}{\tau}}) \quad \text{with} \quad \tau = \frac{L}{R} \quad (18)$$

2) A DC motor convert electrical power in mechanical power. To derive a DC motor physical model some assumptions are made. The system is isolated and do not interact with the surroundings. The armature coil of the motor is represented as a resistor and an inductance. It is also added, in the circuit, a voltage drop proportional to the angular velocity of the coil through the stationary magnetic field. Once the physical model is defined, it is possible to derive the

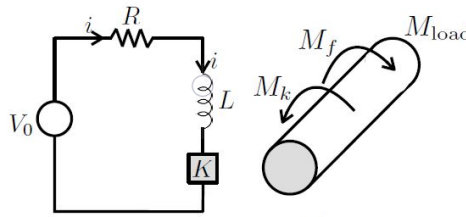


Figure 3: Physical model of a DC motor.

mathematical model Eq.19. In this case it consists of two equations, the first one is related to the equivalent circuit of the physical model, the second one instead, represent the torque balance on the shaft. The following relations instead are the torque generated by friction and torque generated by the coil respectively.

$$\begin{cases} L \frac{di}{dt} + Ri + K\omega = V_0 \\ J \dot{\omega} + b\omega - Ki = M_{load} \end{cases} \quad (19)$$

K is a parameter which depends on the number of winding of the coil, on the length of the winding and on the Resistance of the coil itself. b is the viscous friction coefficient. J is the inertia moment.

$$\begin{aligned} M_f &= b\omega \\ M_k &= Ki \end{aligned} \quad (20)$$

Question 4

1) Write down the Fourier law and show how it is specialized in the case of conduction through a thin plate; discuss the concept of thermal resistance. 2) Report the equation for thermal radiation in case of a) black body and b) real body and discuss them.

The differential form of Fourier's law of thermal conduction shows that the local heat flux density q is equal to the product of thermal conductivity k and the negative local temperature gradient Eq.21.

$$q_h = -k_T(T) \nabla T \quad (21)$$

If a mono-dimensional heat flux is considered, the divergence term becomes a derivative along the direction of the heat flux. The heat flux can be rewritten as follow in Eq.22 where A is the cross sectional area.

$$Q_h = -k_T(T) A \frac{dT}{dx} \quad (22)$$

In case of a thin flat plate of thickness t , Eq.22 can be integrated along the thickness separating the variables (Eq.23).

$$\frac{Qt}{A} = k_T(T) (T_1 - T_2) \quad (23)$$

Considering a constant thermal conductivity it is possible to retrieve a simpler form of Eq.23 and it is:

$$Q = R\Delta T \quad (24)$$

Where R is the conductive resistance. The conductive resistance represents an analogy with the electrical domain. It can be considered in the same way as the resistance in electrical circuits. In case of multiple thermal resistances it is possible to adopt the same procedures of resolution of electrical circuits as deriving the equivalent resistance from two or more resistance either in series or in parallel. Eq.24, similarly to Ohm's law, relates the effort (Temperature) with the Flow (Heat flow). Radiation does not require contact between systems to exchange heat, it also does not require a medium to transmit heat. The heat transmission is done through electromagnetic radiation. A black body is an ideal emitter and using the Stefan-Boltzmann constant it is possible to relate the heat flux radiated to the temperature of the black body and the relation is:

$$Q = \sigma AT^4 \quad (25)$$

where A is the surface of the black body and σ is the Stefan-Boltzmann constant. Since the black body is an idealization, real bodies follow a similar radiation law and it is:

$$Q = \sigma\epsilon AT^4 \quad (26)$$

where ϵ is the emissivity and it is defined as the ratio between the heat flux emitted by a real body over the the heat flux emitted by a black body at the same temperature. If emissivity is equal to 1 the body is a black body.

2 Exercises

Exercise 1

A miniaturized reaction wheel can be modeled as a couple of massive disks, connected with a flexible shaft (Figure 4). The first disk is driven by a rigid shaft, linked to an electric motor. The motor provides a variable torque, while the rigid shaft is subjected to viscous friction, due to motor internal mechanisms. At $t_0 = 0$, the motor provides the torque $T(t) = T_0$.

1) Write down the mathematical model from first principles. 2) Using the data given in the figure caption, and guessing a value for the flexible shaft stiffness k and the viscous friction coefficient b , compute the system response from t_0 to $t_f = 10$ s. 3) Two accelerometers are placed on the two disks recorded samples at 100 Hz, which were saved in the file `samples.txt`; the samples are affected by measurement noise. Determine the value of k and b that allows retracing the experimental data, so avoiding parametric errors.

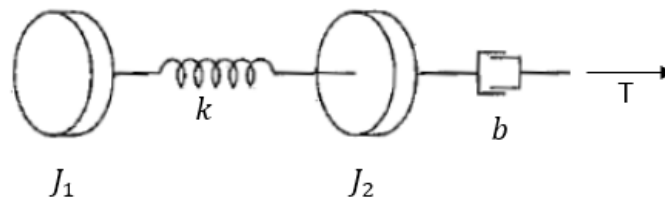


Figure 4: Physical model ($J_1 = 0.2 \text{ kg}\cdot\text{m}$; $J_2 = 0.1 \text{ kg}\cdot\text{m}$; $T_0 = 0.1 \text{ Nm}$).

Starting from the first principle it is possible to retrieve the mathematical model in Eq.27. It is important to highlight that in this exercise it is used the non linear dumper model.

$$\begin{cases} J_1 \ddot{\theta}_1 + k(\theta_1 - \theta_2) = 0 \\ J_2 \ddot{\theta}_2 + k(\theta_2 - \theta_1) + b \text{sign}(\dot{\theta}_2) \dot{\theta}_2^2 = T \end{cases} \quad (27)$$

Using the data in Fig.4 caption and guessing a value of shaft stiffness k equal to 3 and viscous friction coefficient b equal to 0.2. It can be done a simulation of the system behaviour starting from t_0 equal to 0 to t_f equal to 10 s. Fig.5 shows the simulation of the behaviour and it is possible to see that after 3 seconds the oscillations of the two disks converge to zero.

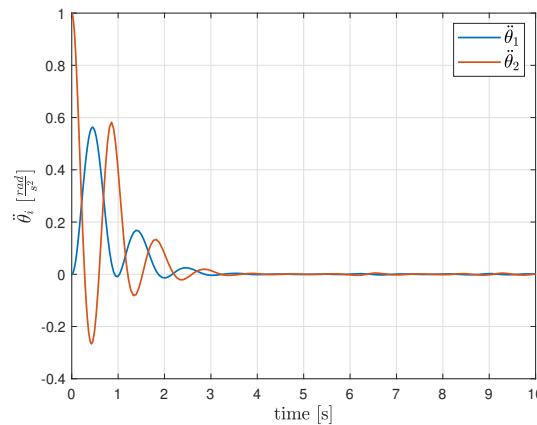
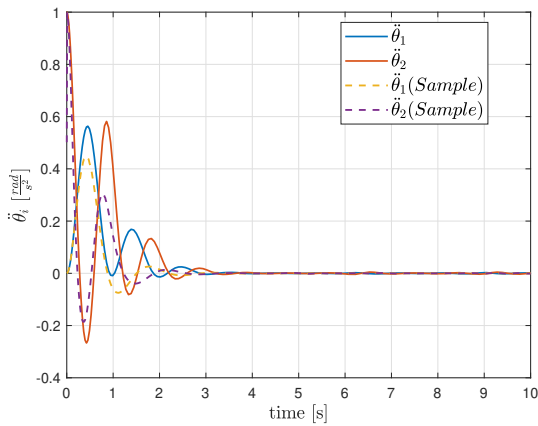


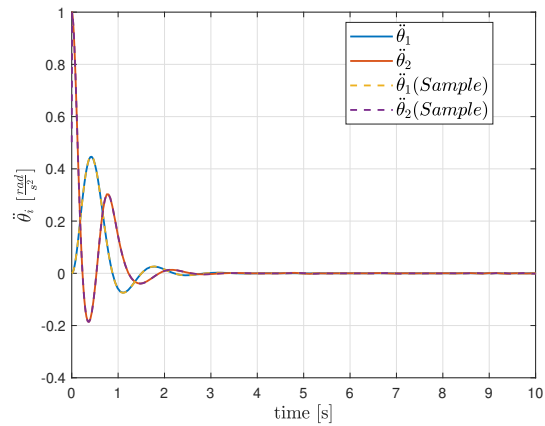
Figure 5: System response assuming $k = 3$ and $b = 0.2$.

The system response is also analyzed using two accelerometers placed on the two disks. The samples are recorded at 100 Hz and collected in the `samples.txt` file. The real values

of k and b are retrieved from the experimental data using the MATLAB `curvefit` function. The solutions obtained are: $b = 2.7121$ and $k = 3.1416$, practically close to the value of the e number and the π number respectively. Fig.6a shows the experimental system response and the simulated system response. In this case the simulated system response values of k and b are equal to the first guessed values of them. Namely $k = 3$ and $b = 0.2$. It is highlighted that the two responses are very different even though they converge to zero after 3 second approximately. Fig.6b instead shows the behaviour of the experimental data against the simulated data. In this case the simulated data are obtained using the value of k and b equal to the ones retrieved from the experimental data themselves. It can be seen that the numerical simulation and the experimental data fit themselves, since they are practically overlapped.



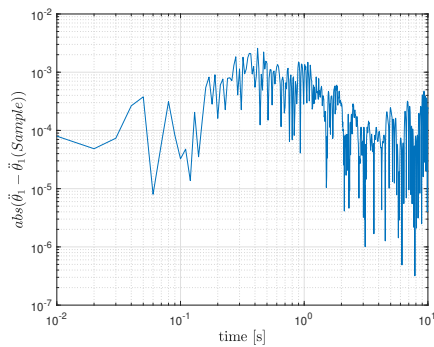
(a) Case with $k = 3$ and $b = 0.2$



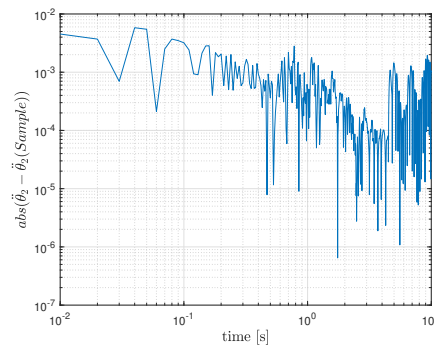
(b) Case with $k = 3.1416$ and $b = 2.7121$

Figure 6: Plots of the simulated system responses against the plots of experimental data collected in `sample.txt`.

Finally, It is analyzed in detail the case of Simulated system response with $k = 3.1416$ $b = 3$. Fig.7 shows the magnitude of errors between $\ddot{\theta}_1$ and $\ddot{\theta}_1(Sample)$ (Fig.7a) and between $\ddot{\theta}_2$ and $\ddot{\theta}_2(Sample)$ (Fig.7b). For both of them the error value is very low with some fluctuation related to computational errors. It is important to highlight that the initial error of $\ddot{\theta}_2$ is high due to the fact that the initial value of the experimental data is equal to 0.5 and the initial value of the simulated data is equal to 1.



(a) Error between $\ddot{\theta}_1$ and $\ddot{\theta}_1(Sample)$



(b) Error between $\ddot{\theta}_2$ and $\ddot{\theta}_2(Sample)$

Figure 7: Magnitude of the error between the experimental data and the simulated data with $k = 3.1416$ and $b = 2.7121$

Exercise 2

The hydraulic system in Figure 8 consists of an accumulator, a check valve, a distributor, an actuator, and a tank, plus delivery and return lines. At $t = t_{-\infty}$, the accumulator contains nitrogen only. To charge it, the nitrogen undergoes an isothermal transformation from $\{p_{N_2}(t_{-\infty}), V_{N_2}(t_{-\infty})\}$ to $\{p_{N_2}(t_0) = p_0, V_{N_2}(t_0) = V_0\}$, t_0 being the initial time. 1) Assuming incompressible fluid, adiabatic discharge of the accumulator, and no leakage in the actuator, write down a mathematical model that allows computing pressures and flow rates in the sections labeled. 2) Considering the distributor command z in Figure 8, carry out a simulation to show the system response in $[t_0, t_f]$. 3) Determine the time t_e that takes the piston to reach the maximum stroke, $x(t_e) = x_{\max}$, starting from $x(t_0) = x_0$, $\dot{x}(t_0) = v_0$.

- Fluid: Skydrol, $\rho = 890 \text{ kg/m}^3$.
- Accumulator: $V_{N_2}(t_{-\infty}) = 10 \text{ dm}^3$, $p_{N_2}(t_{-\infty}) = 2.5 \text{ MPa}$, $p_0 = 21 \text{ MPa}$, adiabatic exponent $\gamma = 1.2$.
- Delivery: Coefficient of pressure drop¹ at accumulator outlet $k_A = 1.12$, coefficient of pressure drop across the check valve $k_{cv} = 2$, diameter of the delivery line $D_{23} = 18 \text{ mm}$; Branch 2–3: Length $L_{23} = 2 \text{ m}$, friction factor² $f_{23} = 0.032$.
- Distributor: Coefficient of pressure drop across the distributor $k_d = 12$, circular cross section, diameter $d_o = 5 \text{ mm}$.
- Actuator: Diameter of the cylinder $D_c = 50 \text{ mm}$, diameter of the rod $D_r = 22 \text{ mm}$, mass of the piston $m = 2 \text{ kg}$, maximum stroke $x_{\max} = 200 \text{ mm}$; Load: $F(x) = F_0 + kx$, $F_0 = 1 \text{ kN}$, $k = 120 \text{ kN/m}$.
- Return: Diameter of the return line $D_r = 18 \text{ mm}$; Branch 6–7: Length $L_{67} = 15 \text{ m}$, friction factor $f_{67} = 0.035$.
- Tank: Pressure $p_T = 0.1 \text{ MPa}$, initial volume $V_T(t_0) = 1 \text{ dm}^3$, coefficient of pressure drop at tank inlet $k_T = 1.12$.
- Initial time: $t_0 = 0$, $x_0 = 0$, $v_0 = 0$; $t_1 = 1 \text{ s}$, $t_2 = 1.5 \text{ s}$; final time $t_f = 3 \text{ s}$.

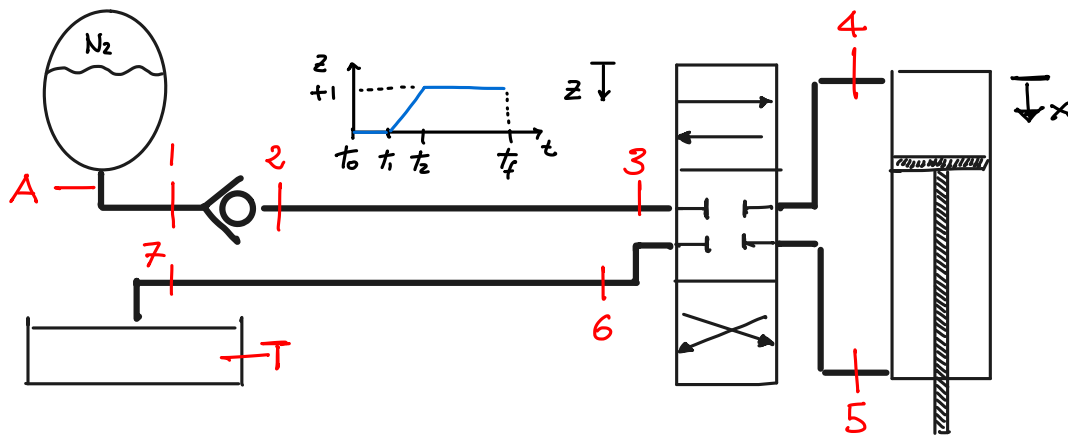


Figure 8: Hydraulic system physical model; assume any other missing data.

¹ $\Delta p = 1/2 k \rho v^2$.

² $\Delta p = f L / D 1/2 \rho v^2$.

It is derived the mathematical model of the system to evaluate pressures and flow rates in the labelled sections. The pressures of the initial part of the hydraulic system are P_A , P_1 , P_2 and P_3 . they are evaluated using the following relations:

$$\begin{aligned} P_A &= P_0 \left(\frac{V_{N2}}{V_{N2i} - V_{acc}} \right)^\gamma \\ P_1 &= P_A - \frac{1}{2} k_A \rho \left(\frac{Q_1}{\pi \frac{D_{23}^2}{4}} \right)^2 \\ P_2 &= P_1 - \frac{1}{2} k_{cv} \rho \left(\frac{Q_2}{\pi \frac{D_{23}^2}{4}} \right)^2 \\ P_3 &= P_2 - \frac{1}{2} f_{23} \frac{L_{23}}{D_{23}} \rho \left(\frac{Q_3}{\pi \frac{D_{23}^2}{4}} \right)^2 \end{aligned} \quad (28)$$

Then the mathematical model related to the last part of the hydraulic system is derived:

$$\begin{aligned} P_7 &= P_{tank} + \frac{1}{2} k_T \rho \left(\frac{Q_7}{\pi \frac{D_{67}^2}{4}} \right)^2 \\ P_6 &= P_7 + \frac{1}{2} f_{67} \frac{L_{67}}{D_{67}} \rho \left(\frac{Q_7}{\pi \frac{D_{67}^2}{4}} \right)^2 \end{aligned} \quad (29)$$

The last part of algebraic equations are related to the distributor.

$$\begin{aligned} P_4 &= P_3 - \frac{1}{2} k_d \rho \frac{Q_3^2}{A_0} \\ P_5 &= P_6 + \frac{1}{2} k_d \rho \frac{Q_7^2}{A_0} \end{aligned} \quad (30)$$

It is important to take into account also the set of equations related to the flow rates:

$$\begin{aligned} Q_4 &= A_4 v \\ Q_5 &= A_5 v \\ Q_1 &= Q_2 = Q_3 \\ Q_6 &= Q_7 \end{aligned} \quad (31)$$

Finally, the differential equations related to the differential variables of the system are derived Eq.32.

$$\begin{aligned} \dot{V}_{acc} &= -Q_A \\ \dot{V}_{tank} &= Q_7 \\ \dot{x}_{piston} &= v_{piston} \\ \dot{v}_{piston} &= \frac{P_4 A_4 - P_5 A_5 - F(x)}{m} \end{aligned} \quad (32)$$

The system of equations formed by Eq.28, Eq.29, Eq.30 and Eq.32 represent the mathematical model of the hydraulic system.

To Simulate the system response it is necessary to integrate and solve the ODEs and the algebraic equations between t_0 and t_f . In this case it is used the ODE23s Matlab function which is a stiff low order integrator. The solutions of the simulation are illustrated in the following plots. Fig.9a shows the motion of the piston inside the cylinder. It can be seen that before the end of the simulation, the piston reach the maximum stroke. Fig.9b represents the velocity of the piston during the simulation. The velocity is zero between $t = 0$ and t_0 , since the accumulator valve is closed. When the valve is opened velocity rise up to 0.35 and then goes down. When the piston reach the maximum stroke the velocity turns zero.

Fig.10c and Fig.10a illustrate the behaviour of the pressures in label in the accumulator, label 1, 2, 3 and the last part of the hydraulic system. P_A , P_1 , P_2 and P_3 experience a similar behaviour due to the low pressure drop. Then, Fig.10b shows the pressure variations inside the cylinder.

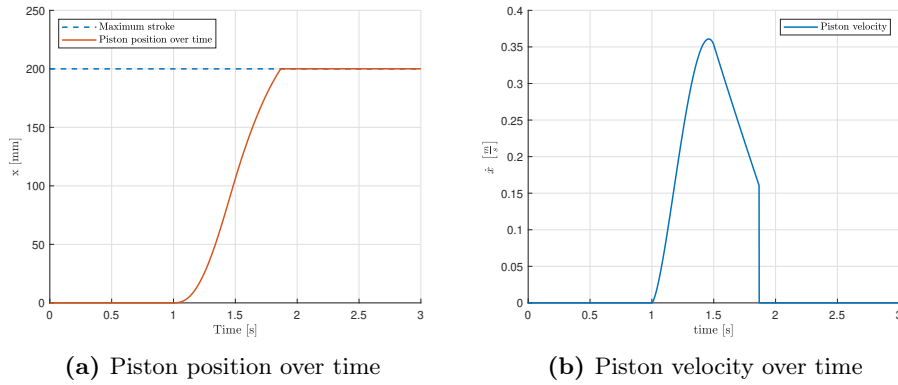


Figure 9: Position and velocity of the piston over time.

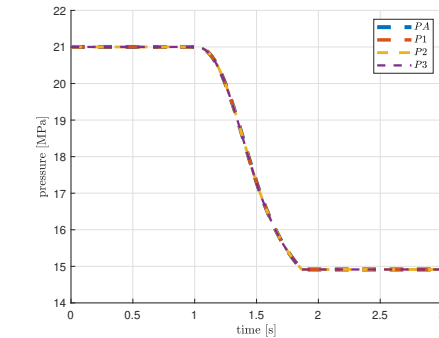
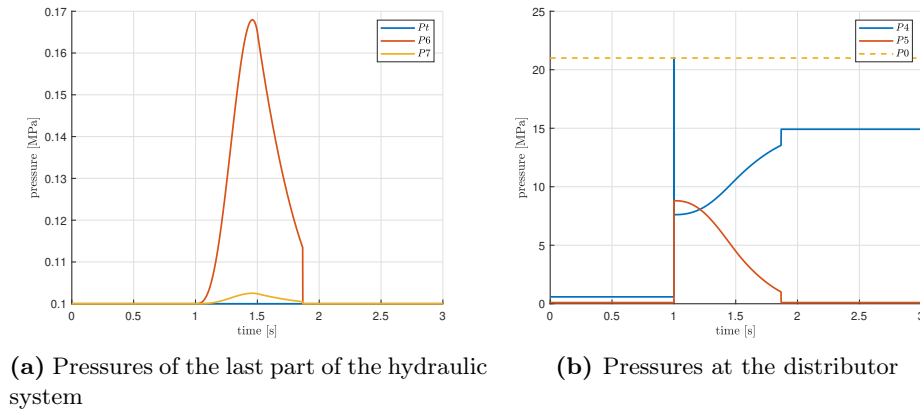
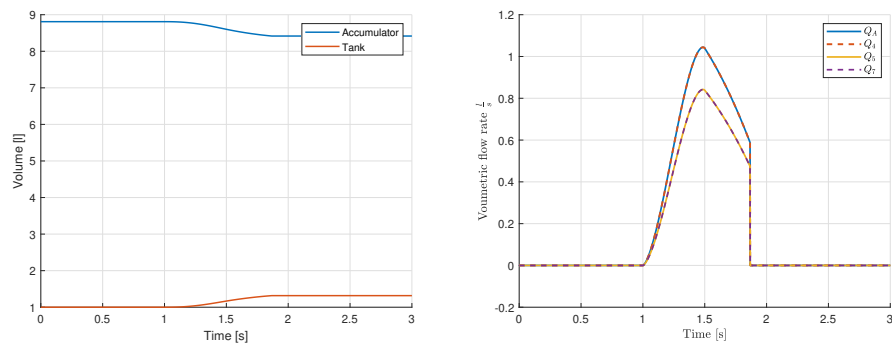


Figure 10: Plots of pressures of the hydraulic system .

Fig.11a shows the variation of volume inside the accumulator and inside the tank. The volume of the first decrease and the volume of the second increase. The last plot shows the variation of the flow rate during the simulation over time Fig.11b. Finally, it is determined the time that takes the piston to reach the maximum stroke t_e which is equal to 1.8671 s.



(a) Accumulator and Tank variation of volume (b) low rates of the system over time

Figure 11

Exercise 3

Consider the ideal physical model network shown in Figure 12. The switch has been open for a long time. The capacitor is charged and has a voltage drop between its ends equal to 1 V. Then, at $t = 0$, the switch is closed. 1) Plot the subsequent time history of the voltage V_C across the capacitor. 2) Assume a voltage source characterized by $v(t) = \sin(2\pi ft) \arctan(t)$ having the positive terminal downward inserted in place of the switch. What is in this case the voltage history across the capacitor?

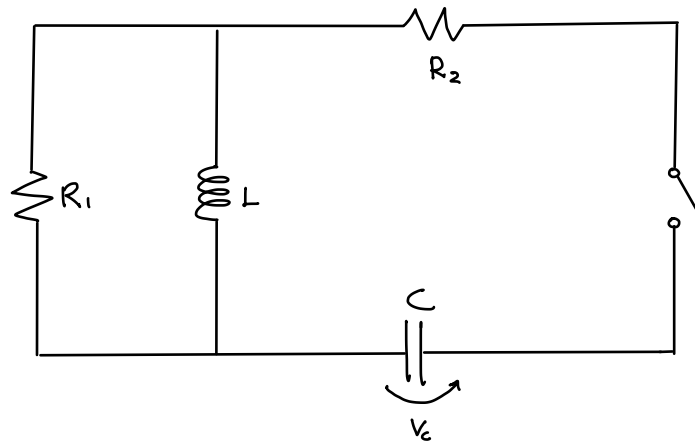


Figure 12: Circuit physical model ($R_1 = 1000 \Omega$; $R_2 = 100 \Omega$; $L = 1 \text{ mH}$; $C = 1 \text{ mF}$; $f = 5 \text{ Hz}$.)

From the physical model network in Fig.12 it is possible to retrieve the mathematical model using the Kirchhoff's laws. Since it is an RLC circuit, the equation which describe the V_c history is a second order ODE and it is shown in Eq.33.

The capacitor voltage history after the switch is closed is shown in Fig.13. It can be seen that the voltage decreases over time converging to the zero value after 0.5 s. This solution is obtained by converting the second order ODE in Eq.33 in a state space representation. Then, the state space system is integrated using the ODE23t Matlab function. ODE23t is a function which integrate moderately stiff systems using the trapezoidal rule. It is found, after a trial and error approach, that this system is a moderate stiff ODE and for this reason it is necessary to use an integrator which can solve stiff systems.

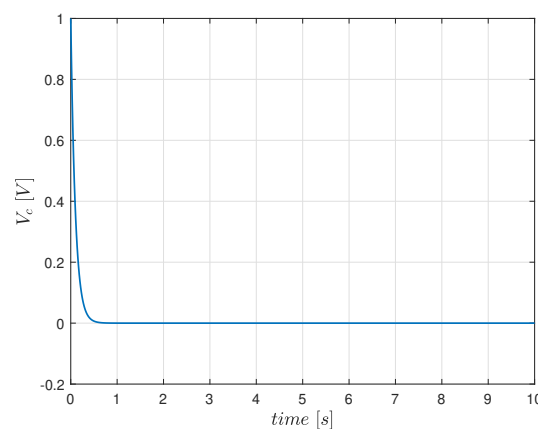


Figure 13: Voltage history of the capacitor

$$\ddot{V}_c + \frac{L + R_1 R_2 C}{(R_1 + R_2) CL} \dot{V}_c + \frac{R_1}{(R_1 + R_2) CL} V_c = 0 \quad (33)$$

The same approach is used for the second part of the exercise. In this case a voltage source is taken into account in place of the switch. From this new physical model network it is possible to derive the mathematical model using the kirchoff's laws and the solution is shown in Eq.14. The left hand side of the equaiton is identical to Eq.33 but the contribution of the voltage source is in the right hand side of the equation.

$$\ddot{V}_c + \frac{L + R_1 R_2 C}{(R_1 + R_2) CL} \dot{V}_c + \frac{R_1}{(R_1 + R_2) CL} V_c = \frac{R_1 v(t) + L \dot{v}(t)}{(R_1 + R_2) LC} \quad (34)$$

The ODE in Eq.14 is converted in a state space system and then integrated using the `ODE23t` Matlab function. Also in this case the ODE is moderately stiff. The capacitor voltage history is then plotted in Fig.14. Initially there is a decrease of the capacitor voltage, as experienced in the previous case. Then the voltage source generate an oscillation around $0V$ with an increasing amplitude. At 10 seconds, the final time of the simulation, the amplitude is between $0.4V$ and $-0.4V$ approximately.

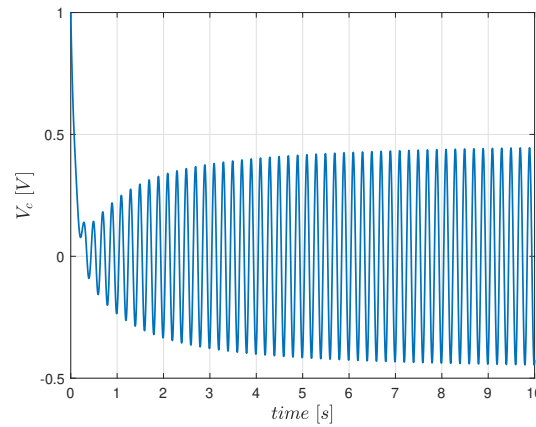


Figure 14: Voltage history of the capacitor

Exercise 4

The rocket engine in Figure 15 is fired in laboratory conditions. With reference to Figure 15, the nozzle is made up of an inner lining (k_1), an inner layer having specific heat c_2 and high conductivity k_2 , an insulating layer having specific heat c_4 and low conductivity k_4 , and an outer coating (k_5). The interface between the conductor and the insulator layers has thermal conductivity k_3 . 1) Select the materials of which the nozzle is made of³, and therefore determine the values of k_i ($i = 1, \dots, 5$), c_2 , and c_4 . Assign also the values of ℓ_i ($i=1, \dots, 5$), L , and A in Figure 15. 2) Derive a physical model and the associated mathematical model using one node per each of the five layers and considering that only the conductor and insulator layers have thermal capacitance. The inner wall temperature, T_i , as well as the outer wall temperature, T_o , are assigned. 3) Using the mathematical model at point 2), carry out a dynamic simulation to show the temperature profiles across the different sections. At initial time, $T_i(t_0) = T_o(t) = 20$ C°. When the rocket is fired, $T_i(t) = 1000$ C°, $t \in [t_1, t_f]$, following a ramp profile in $[t_0, t_1]$. Integrate the system using $t_1 = 1$ s and $t_f = 60$ s. 4) Repeat the simulation in point 3) using a mathematical model implementing two nodes for the conductor and insulator layers.

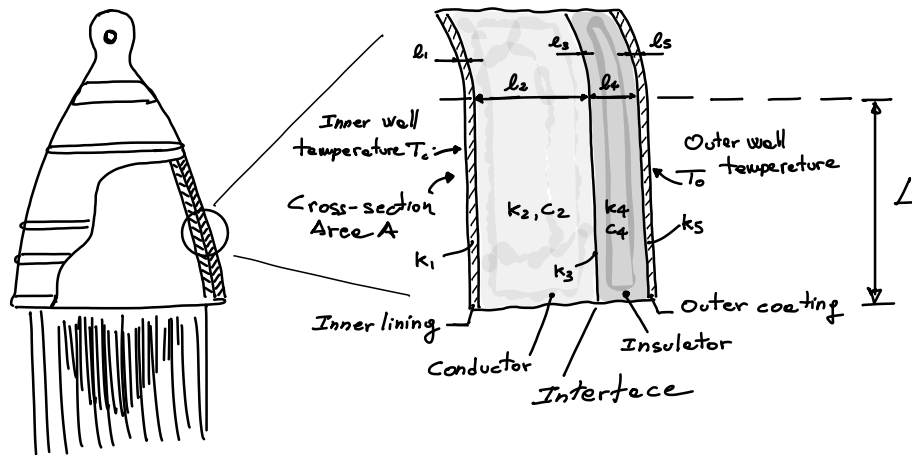


Figure 15: Real thermal system.

In this exercise it is necessary to assume several values depending on the materials of which the nozzle is made of. It is supposed that the inner lining is made of a NARloy, the conductor layer is supposed to be made of a copper alloy, the insulator layer is made of a nickel alloy with low conductivity and the outer coating is made of a nickel superalloy (718). Then the inner component properties are collected in Tab.2.

Table 2: Missing values.

Data		
$k_1 = 400 \frac{W}{mK}$	$l_1 = 0.01$ m	$R_3 = 0.07 \frac{m^2K}{W}$
$k_2 = 385 \frac{W}{mK}$	$l_2 = 0.05$ m	$c_2 = 385 \frac{J}{kgK}$
$k_4 = 76 \frac{m^2K}{W}$	$l_4 = 0.03$ m	$c_4 = 456 \frac{J}{kgK}$
$k_5 = 25 \frac{W}{mK}$	$l_5 = 0.01$ m	

³The interface layer is not made of a physically existing material, though it produces a thermal resistance. For this layer, the value of the thermal resistance R_3 can be directly assumed, so avoiding to choose k_3 and ℓ_3 .

The values selected are to be intended as reference value since they may vary with respect to the temperature. It is important to specify that the R_3 value is directly assumed since the interface layer is not made of a physically existing material. It is firstly derived a physical model using the multiple lumped parameter approach where the continuum is replaced with equivalent thermal circuit with lumped capacitance and resistance elements. The equivalent thermal circuit and the nodes position are shown in Fig.16. Then is developed the mathematical model where

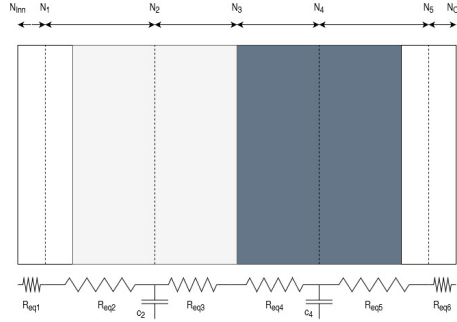


Figure 16: Physical model with 7 nodes.

T_i are the temperatures at each node and R_{eq_i} are the equivalent thermal resistances between two nodes. Eq.35 are first order ODEs due to the fact that conductor and insulator layers have also thermal capacitance, while the other three nodes (Eq.36) are located in layers where thermal capacitance is neglected.

$$\begin{cases} \dot{T}_2 = \frac{1}{c_2} \left(\frac{T_1 - T_2}{R_{eq2}} - \frac{T_2 - T_3}{R_{eq3}} \right) \\ \dot{T}_4 = \frac{1}{c_4} \left(\frac{T_3 - T_4}{R_{eq4}} - \frac{T_4 - T_5}{R_{eq5}} \right) \end{cases} \quad (35)$$

$$\begin{cases} T_1 = \left(\frac{T_{Inn}}{R_{eq1}} + \frac{T_2}{R_{eq2}} \right) \cdot \frac{1}{\frac{1}{R_{eq1}} + \frac{1}{R_{eq2}}} \\ T_3 = \left(\frac{T_2}{R_{eq3}} + \frac{T_4}{R_{eq4}} \right) \cdot \frac{1}{\frac{1}{R_{eq3}} + \frac{1}{R_{eq4}}} \\ T_5 = \left(\frac{T_4}{R_{eq5}} + \frac{T_{Out}}{R_{eq6}} \right) \cdot \frac{1}{\frac{1}{R_{eq5}} + \frac{1}{R_{eq6}}} \end{cases} \quad (36)$$

Finally, the system of ODEs is integrated over time and then all the temperature profiles are collected. Fig.17 shows the temperature trend of each node along time. The N_{Inn} temperature

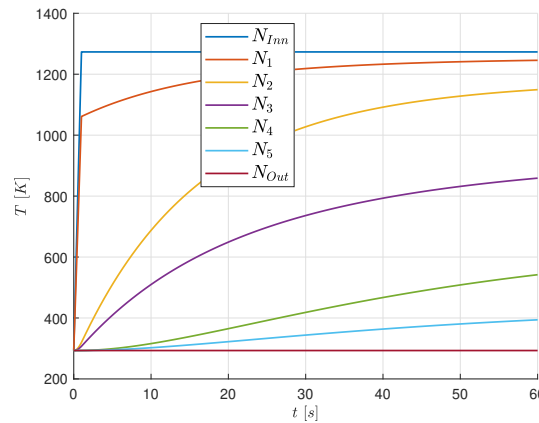


Figure 17: Nodes temperature over time

follows the ramp profile of the ignition. The first node, which is inside the inner lining, follows a

similar behaviour of the internal node while, the other nodes experience a smoother variation of temperature over time. The same procedure is done for the second simulation but in this case two nodes are used in the conductor layer and two nodes are used in the insulator layer. Fig.19 shows the new physical model by using the lumped parameter approach with the equivalent thermal circuit.

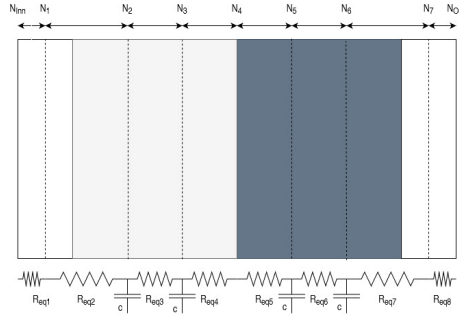


Figure 18: Physical model with 9 nodes.

From the physical model the mathematical model is retrieved which is displayed in Eq.37 and Eq.38. Given the presence of two nodes in the conductor layer and two nodes in the insulator layer, there are four ODEs representing the system.

$$\begin{cases} \dot{T}_2 = \frac{1}{0.5 \cdot c_2} \left(\frac{T_1 - T_2}{R_{eq2}} - \frac{T_3 - T_2}{R_{eq3}} \right) \\ \dot{T}_3 = \frac{1}{0.5 \cdot c_2} \left(\frac{T_2 - T_3}{R_{eq3}} - \frac{T_3 - T_4}{R_{eq4}} \right) \\ \dot{T}_5 = \frac{1}{0.5 \cdot c_4} \left(\frac{T_4 - T_5}{R_{eq5}} - \frac{T_5 - T_6}{R_{eq6}} \right) \\ \dot{T}_6 = \frac{1}{0.5 \cdot c_4} \left(\frac{T_5 - T_6}{R_{eq6}} - \frac{T_6 - T_7}{R_{eq7}} \right) \end{cases} \quad (37)$$

$$\begin{cases} T_1 = \left(\frac{T_{Inn}}{R_{eq1}} + \frac{T_2}{R_{eq2}} \right) \cdot \frac{1}{\frac{1}{R_{eq1}} + \frac{1}{R_{eq2}}} \\ T_3 = \left(\frac{T_2}{R_{eq3}} + \frac{T_4}{R_{eq4}} \right) \cdot \frac{1}{\frac{1}{R_{eq3}} + \frac{1}{R_{eq4}}} \\ T_5 = \left(\frac{T_4}{R_{eq5}} + \frac{T_{Out}}{R_{eq6}} \right) \cdot \frac{1}{\frac{1}{R_{eq5}} + \frac{1}{R_{eq6}}} \end{cases} \quad (38)$$

Known the mathematical model Matlab code is implemented in order to integrate the ODEs over time. This code is based on the ODE45 Matlab function. The solutions are plotted in Fig.19

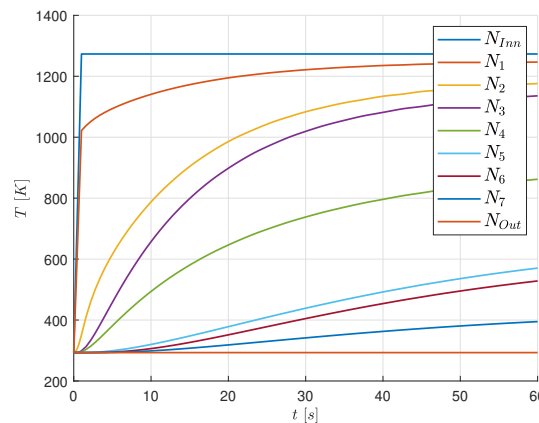


Figure 19: Nodes temperature over time